of $1^{-\cdot}$ on **1** would not necessarily lead to the same nuclear arrangement as dimerization of $1^{-\cdot}$ and the question of the structure of the chain carrier and its chemical behavior on electron transfer must remain open.

Experimental Section

Materials. 9-Diazofluorene (**1**) was prepared as previously described.[13] The phosphazine **7** was prepared by reaction of **1** with triphenylphosphine in acetonitrile solution; recrystallized from chloroform/ether it had mp 209-210 °C (lit.[14] mp 209-210 °C). Acetonitrile and tetraethylammonium tetrafluoroborate were purified commercial samples; solutions (0.1 M) were dried immediately prior to addition of **1** or **7** by filtration through a 20-cm column of activated alumina (Woelm, N. Super).

DCV and DLSV Experiments. The instrumentation was as described in earlier publications.[15] The working elecrode was a platinum disc 0.4 mm in diameter and the reference electrode Ag/Ag^+ (0.01 M in CH_3CN). Solutions of **1** (5 mM) or **7** (1.5 mM) containing 9,10-dimethylphenazine (0.67 mM) were studied. The starting potential for experiments on **1** was -2.5 V and the scan was +2.5 V at intervals of 60 s; experiments on **7** started at a potential of -3.0 V and the scan was +3.0 V. After differentiation of the current-voltage curves and analog to digital conversion, the peak height ratios were evaluated with an on-line computer. The standard deviations on the values was usually 1% of the quoted value.

Registry No. 1, 832-80-4; **7**, 751-35-9; triphenylphosphine, 603-35-0.

(13) Staudinger, H.; Kupfer, O. *Ber.* **1911**, *44*, 2197.
(14) Staudinger, H.; Meyer, J. *Helv. Chim. Acta* **1919**, *2*, 619.
(15) See, for example: Parker, V. D. *Acta Chem. Scand.* **1981**, *B35*, 349.

Structural and Magnetic Study of $Ni_2(EDTA)(H_2O)_4,2H_2O$. Alternating Landé Factors in a Two-Sublattice 1D System

E. Coronado,[⊥] M. Drillon,*[⊥] A. Fuertes,[‡] D. Beltran,[‡] A. Mosset,[§] and J. Galy[§]

Contribution from the Département Science des Matériaux, E.N.S.C.S., 67008 Strasbourg, France, the Departamento de Quimica Inorganica, Universidad de Valencia, Valencia, Spain, and the Laboratoire de Chimie de Coordination, du C.N.R.S., 31400 Toulouse, France.
Received January 25, 1985

Abstract: We report on the structure and magnetic behavior of the chain complex $Ni_2(EDTA)(H_2O)_4,2H_2O$ characterized by two different sites for Ni(II) ions. These are coordinated either to the EDTA ligand or to oxygen atoms belonging to carboxylate groups of the EDTA and four water molecules; they are connected in order to form alternating zigzag chains. The magnetic behavior is discussed in terms of regular spin-1 chain with alternating Landé factors $S(g_a)$-$S(g_b)$-$S(g_a)$.... Both Heisenberg and Ising exchange models are shown to describe the experimental data down to about 10 K, for a coupling constant $J \simeq -8.3$ K. However, due to local anisotropy effects, the latter gives a better agreement with experiment at lower temperature.

Thermodynamics of one-dimensional Heisenberg systems was first investigated by Bonner and Fischer[1] in a pioneering work on the spin $^1/_2$ chain and extended by Weng[2] and De Neef[3] to higher spin networks. Further, the $S = {}^1/_2$ dimerized chain involving two exchange parameters was solved by Duffy and Barr[4] by means of the same computational procedure. Results of these studies were extensively confronted with experiment, so that they constitute today current methods when determining the exchange constants in 1D materials.[5] When discrepancies occur at low temperatures these are usually attributed either to interchain couplings or to distortions of the local environments leading to a splitting of the low-lying levels. Unfortunately, a complete treatment of such effects is not available so far.

Recently, we have shown that the alternation of magnetic sites (two-sublattice chain) due to distinct local symmetries or distinct metal ions causes equally drastic effects on the temperature dependence of the effective moment.[6-8] Mention, in particular, a minimum of the curve $\chi T = f(T)$ at intermediate $kT/|J|$ value and a divergence when approaching absolute zero, according to a power law variation. Such a behavior was shown to be the signature of a ferrimagnetic short-range ordering.

In this paper, we discuss the structure and magnetic properties of the $Ni_2EDTA(H_2O)_4,2H_2O$ complex showing two distinct nickel(II) sublattices connected in order to form infinite chains A-B-A-B.... From an electronic viewpoint, the site symmetry alternation results in alternating Landé factors, and consequently in alternating moments. Then, the problem is to be compared to the previously investigated one on the ordered bimetallic chains with two distinct spin sublattices. The behavior of the title compound will be discussed here on the basis of Heisenberg and Ising chain models including a g alternation.

Table I. Crystallographic Data and Conditions for Data Collection and Refinement

1. Physical and Crystallographic Data	
formula: $Ni_2(C_{10}N_2O_8)(H_2O)_4,2H_2O$	molecular weight: 513.73
crystal system: orthorhombic	space group: $Pna2_1$
a = 14.370 (25) Å	V = 1821.2 Å^3
b = 9.638 (5) Å	Z = 4
c = 13.150 (5) Å	
ρ_{expl} = 1.86 (2) g·cm^{-3}; ρ_X = 1.87 g·cm^{-3}	
2. Data Collection	
temperature: 20°C	
radiation: molybdenum	λKα = 0.71069 Å
monochromatization: oriented graphite crystal	
crystal-detector distance: 208 mm	
detector window: height* = 4 mm; width* = 4 mm	
take-off angle: 2°	
scan mode: θ-2θ	
maximum Bragg angle: 27°	
scan angle: $\Delta\theta = \Delta\theta_0 + B \tan\theta$; $\Delta\theta_0$ = 0.90, B = 0.347	
values determining the scan-speed: SIGPRE* = 0.75; SIGMA* = 0.018; VPRE* = 10°/mn; TMAX* = 90 s	
controls: intensity	orientation
reflections: 00$\bar{4}$, $\bar{4}$00, 0$\bar{6}$0;	060, 415, 008
periodicity: 3600 s; 100 reflections	
3. Conditions for Refinement	
reflections for the refinement of the cell dimensions: 25	
recorded reflections: 2291	
utilized reflections: 1956 with $I \geq 3\sigma(I)$	
refined parameters: 253	
reliability factors: $R = \sum\|k\|F_o\| - \|F_c\|/\sum k F_o$ = 0.033; $R_w = [\sum w(k\|F_o\| - \|F_c\|)^2/\sum wk^2F_o^2]^{1/2}$ = 0.040	

⊥ Département Science des Matériaux, E.N.S.C.S.
‡ Universidad de Valencia.
§ Laboratoire de Chimie de Coordination, du C.N.R.S.

0002-7863/86/1508-0900$01.50/0

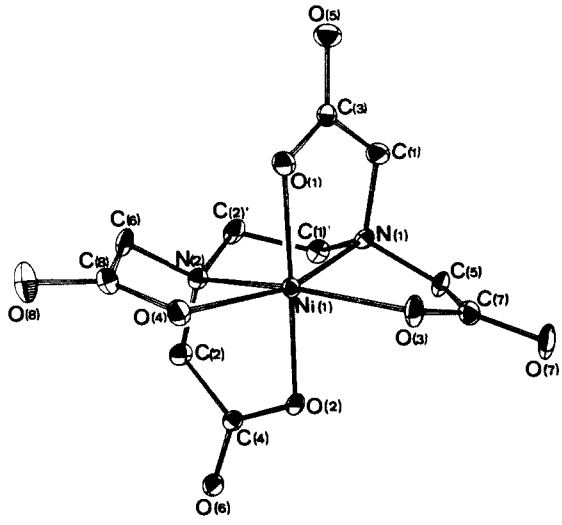

Figure 1. Sketch of the Ni(1)–EDTA moiety.

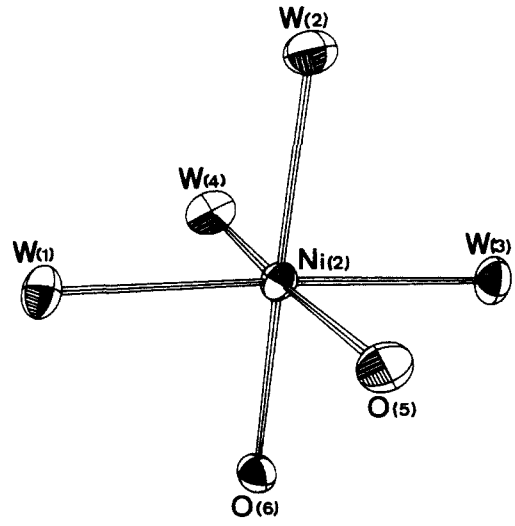

Figure 2. Sketch of the Ni(2) metallic site environment.

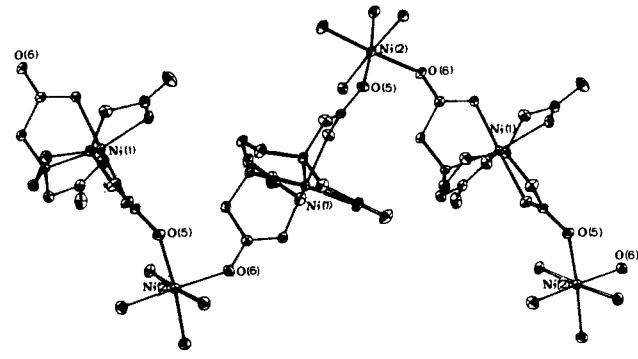

Figure 3. Geometry of the alternating Ni(EDTA)–$Ni(H_2O)_4$ chain.

Experimental Section

Crystallographic Study. The title compound (hereafter abbreviated as (NiNi)) has been prepared by a previously described procedure.[9] This complex belongs to the isostructural series $MM'(EDTA)(H_2O)_4,2H_2O$ (with M,M' = Mn(II), Ni(II), Co(II), Cu(II), Zn(II))[9] that crystallizes in an orthorhombic system with a $Pna2_1$ space group.[10] Cell constants and corresponding standard deviations, listed in Table I, were derived by least-squares refinement of the setting of 25 reflections automatically centered on a CAD4 Enraf-Nonius computer-controlled diffractometer. The crystal selected for the data collection was a needle-shaped prism of dimensions 0.15 × 0.20 × 0.90 mm characterized by boundary faces (110), (1$\bar{1}$0), (0$\bar{1}\bar{1}$), and (011). The crystal was mounted with (001) approximately along the spindle axis. Data were collected at 20 °C by the θ–2θ scan method with graphite Mo Kα monochromatized radiation and following the scheme of Table I, fully described elsewhere.[11]

The structure was refined from the atomic positions of the (ZnZn) complex[10] as starting data by full-matrix least-squares techniques (in addition to local programs for the CII Iris 80 computer, local modifications of the following programs were employed: Zalkin's Fourier program, Ibers and Doeden's NUCLS program, Busing, Martin, and Levy's ORFFE program,[12] and Johnson's ORTEP program[13]). The quantity minimized was $w(F_o - |F_c|)^2$, where F_o and F_c are the observed and calculated structure factor amplitudes and where the weights w are taken as $4F_o^2/\sigma(F_o)^2$. The agreement indices are defined in Table I. Values of the atomic scattering factors and anomalous terms for the nickel atom were chosen from Cromer and Waber tables.[14]

All the ligand hydrogen atoms were located on a difference Fourier map. The positions of hydrogen atoms of the water molecules w(5) and w(6), difficult to define reliably, were deleted from the model. The hydrogen atoms, with isotropic thermal parameter, were introduced as fixed contribution in the calculations.

We have reported, in Table II, the atomic parameters together with their standard deviations as derived from the inverse matrix.

Magnetic Measurements. The magnetic susceptibilities were performed in the range 4–100 K with a pendulum-type apparatus equipped with a He cryostat. The uncertainty on the data is lower than 0.1 K for temperatures and 2×10^{-5} emu·mol^{-1} for susceptibilities.

All magnetic measurements reported hereafter correspond to corrected values for the diamagnetic contribution estimated to be -170×10^{-6} emu·mol^{-1} from Pascal's tables.

Structural Results

The crystal structure of $Ni_2(EDTA)(H_2O)_4,2H_2O$ is built up from two different subunits:

The former deals with the Ni(1) metallic site hexacoordinated to the EDTA ligand (Figure 1). Owing to the constraints exerted by the ligand, the $Ni(1)N_2O_4$ octahedron is highly distorted with a deviation angle O(3)–Ni(1)–O(4) rising up to 22.7°; the largest deviations are observed in the coordination plane corresponding to the ethylenediamine ring. As indicated in Table III, the Ni(1)–O and Ni(1)–N bond lengths do not differ much from the average value of 2.069 Å. The mean distance of metal–nitrogen (2.084 Å) is slightly shorter in the title compound than in most of the other complexes of the series, according to the smallest hexacoordinated ionic radius of the nickel ion ((CoCo) = 2.16 Å, (ZnZn) = 2.113 Å, (MnCo) = 2.151 Å, (MgZn) = 2.154 Å, (MnCu) = 2.042 Å.[15,16] Interatomic distances and angles within the EDTA ligand are in the usual range. The asymmetry of the bridging carboxylate groups corresponds to what is expected, indicating a strong interaction with the "chelated" Ni(1) site.

The second subunit is less distorted; it corresponds to Ni(2) metallic sites surrounded by two oxygen atoms and four water molecules. The oxygens O(5) and O(6) belong to two different (Ni(1)EDTA) units (Figure 2). Bond lengths and bond angles are quite normal, even though the values look more widespread

(1) Bonner, J. C.; Fischer, M. E. *Phys. Rev.* **1964**, *135A*, 640.
(2) Weng, C. Y. Ph.D. Thesis, Carnegie Institute of Technology, 1968.
(3) De Neef, T. *Phys. Rev.* **1976**, *B13*, 4141.
(4) Duffy, W.; Barr, K. P. *Phys. Rev.* **1968**, *165*, 647.
(5) See for instance: Hatfield, W. E. In "Extended Linear Chain Compound"; Miller, J. S., Ed.; Plenum Press: New York and London, 1983; Vol. 3.
(6) Drillon, M.; Coronado, E.; Beltran, D.; Georges, R. *Chem. Phys.* **1983**, *79*, 449.
(7) Drillon, M.; Gianduzzo, J. C.; Georges, R. *Phys. Lett.* **1983**, *96A*, 413.
(8) Drillon, M.; Coronado, E.; Beltran, D.; Georges, R. *J. Appl. Phys.* **1985**, *57*, 3353.
(9) Escriva, E.; Fuertes, A.; Beltran, D. *Transition Met. Chem.* (*Weinheim, Ger.*) **1984**, *9*, 184.
(10) Pozhidaev, A. I.; Polynova, T. M.; Porai-Koshits, M. A.; Neronova, M. N. *Zh. Struk. Khim.* **1973**, *14*, 570.
(11) Mosset, A.; Bonnet, J. J.; Galy, J. *Acta Crystallogr.* **1977**, *B33*, 2639.
(12) Busing, W. R.; Martin, K. O.; Levy, H. A., ORFEE Report ORNL-TM-306, 1964, Oak Ridge National Laboratory, TN.
(13) Johson, C. K., ORTEP Report ORNL-3794, 1965, Oak Ridge National Laboratory, TN.
(14) Cromer, D. T.; Waber, J. T. "International Tables for X-ray Crystallography"; Kynoch Press: Birmingham, 1974; Vol. 4, Table 2.2.A.
(15) Mc Candlish, E. F. K.; Michael, T. K.; Neal, J. A.; Lingafelter, E. C.; Rose, N. J. *Inorg. Chem.* **1978**, *17*, 1383.
(16) Solans, X.; Gali, S.; Font-Altaba, M.; Oliva, J.; Herrera, J. *Acta Crystallogr.* **1983**, *C39*, 435.

Table II. Final Atomic Parameters. The EDTA Hydrogen Atoms Are Labeled H_1 to H_{62} and the Water Hydrogen Atoms H_{111} to H_{162}[a]

atom	x	y	z	B_{11} or B (Å^2)	B_{22}	B_{33}	B_{12}	B_{13}	B_{23}
Ni(1)	0.06066 (5)	0.18166 (8)	1/4	1.35 (3)	4.28 (8)	1.26 (4)	−0.05 (4)	−0.06 (3)	0.06 (6)
Ni(2)	0.23596 (5)	0.69014 (8)	0.22894 (8)	1.69 (3)	4.25 (8)	1.51 (4)	0.12 (4)	−0.01 (3)	0.03 (6)
O(1)	0.0012 (3)	−0.0097 (5)	0.2446 (4)	1.8 (2)	4.7 (4)	2.7 (3)	0.1 (2)	0.4 (2)	−0.4 (4)
O(2)	0.1235 (3)	0.3759 (5)	0.2529 (4)	2.7 (2)	6.0 (5)	1.0 (2)	−1.1 (3)	−0.2 (2)	0.0 (3)
O(3)	0.0721 (4)	0.1777 (6)	0.4058 (4)	2.6 (3)	8.7 (7)	1.1 (2)	0.6 (3)	−0.1 (2)	0.1 (3)
O(4)	0.1734 (3)	0.0901 (5)	0.1778 (4)	1.6 (2)	6.9 (6)	1.8 (3)	0.0 (3)	−0.2 (2)	0.0 (3)
O(5)	−0.1313 (3)	−0.1229 (5)	0.2589 (4)	2.1 (2)	5.5 (5)	3.4 (3)	−0.9 (3)	−0.1 (2)	0.0 (4)
O(6)	0.1937 (3)	0.5207 (5)	0.1459 (4)	2.9 (3)	4.4 (5)	2.2 (3)	−0.6 (3)	0.2 (2)	−0.1 (3)
O(7)	0.0188 (4)	0.2927 (7)	0.5396 (4)	3.1 (3)	14.3 (9)	1.2 (3)	0.5 (4)	0.2 (2)	−1.2 (4)
O(8)	0.2128 (4)	0.0064 (6)	0.0250 (4)	3.7 (3)	8.5 (7)	2.2 (3)	2.3 (4)	1.0 (3)	0.9 (4)
W(1)	0.1845 (3)	0.5999 (6)	0.3619 (4)	2.1 (2)	7.4 (6)	1.7 (3)	−0.5 (3)	0.1 (2)	0.1 (3)
W(2)	0.2622 (4)	0.8794 (5)	0.2965 (4)	2.7 (2)	5.6 (5)	3.7 (3)	0.3 (3)	0.1 (2)	−1.1 (4)
W(3)	0.2916 (4)	0.7704 (5)	0.0963 (4)	2.6 (2)	6.4 (6)	2.7 (3)	0.2 (3)	0.9 (2)	1.1 (5)
W(4)	0.1059 (4)	0.7653 (6)	0.1906 (4)	2.3 (2)	7.6 (6)	3.1 (3)	0.8 (3)	−0.8 (2)	−0.8 (4)
W(5)	0.4746 (5)	0.8568 (8)	0.3446 (6)	4.9 (4)	13.8 (10)	7.1 (5)	−1.2 (5)	1.2 (4)	−3.4 (6)
W(6)	0.3031 (5)	0.4830 (7)	−0.0281 (5)	4.8 (4)	10.1 (8)	2.8 (3)	−1.8 (5)	0.9 (3)	−0.8 (4)
N(1)	−0.0732 (4)	0.2444 (6)	0.2854 (4)	1.8 (2)	4.1 (6)	1.7 (3)	0.0 (3)	−0.5 (2)	−0.4 (3)
N(2)	0.0320 (4)	0.2396 (6)	0.0994 (4)	1.7 (3)	4.7 (6)	1.8 (3)	0.3 (3)	−0.4 (2)	−0.1 (4)
C(1)″	−0.1005 (5)	0.3327 (8)	0.1982 (5)	2.2 (3)	5.4 (8)	2.7 (4)	0.8 (4)	−0.4 (3)	−0.1 (4)
C(2)″	−0.0703 (5)	0.2625 (9)	0.0982 (5)	2.2 (3)	7.4 (9)	2.2 (4)	0.7 (5)	−1.0 (3)	−1.1 (5)
C(1)	−0.1321 (5)	0.1178 (8)	0.2956 (6)	1.8 (3)	5.4 (7)	3.2 (4)	−0.3 (4)	0.3 (3)	−0.4 (5)
C(2)	0.0847 (5)	0.3666 (8)	0.0750 (5)	3.1 (4)	6.3 (8)	1.5 (3)	−1.0 (4)	−0.7 (3)	0.6 (4)
C(3)	−0.0850 (4)	−0.0142 (6)	0.2623 (5)	2.1 (3)	4.7 (6)	1.3 (3)	−0.3 (3)	−0.2 (3)	0.3 (4)
C(4)	0.1395 (4)	0.4260 (7)	0.1655 (5)	1.7 (3)	3.9 (7)	2.0 (4)	0.1 (4)	−0.2 (3)	−0.1 (4)
C(5)	−0.0637 (5)	0.3200 (8)	0.3834 (5)	2.1 (3)	6.9 (8)	1.6 (4)	0.7 (4)	−0.1 (3)	−1.5 (5)
C(6)	0.0657 (5)	0.1198 (8)	0.0391 (5)	2.7 (3)	6.8 (8)	1.3 (3)	0.4 (5)	−0.2 (3)	−1.1 (4)
C(7)	0.0142 (5)	0.2575 (8)	0.4476 (5)	2.1 (3)	6.6 (8)	1.8 (3)	−0.4 (4)	−0.1 (3)	0.3 (5)
C(8)	0.1583 (5)	0.0689 (7)	0.0822 (5)	1.9 (3)	5.3 (7)	2.0 (4)	0.3 (4)	0.3 (3)	0.4 (4)
H(1)	−0.163	0.345	0.198	2.5					
H(2)	−0.073	0.417	0.203	2.5					
H(3)	−0.086	0.318	0.044	2.5					
H(4)	−0.100	0.181	0.091	2.5					
H(11)	−0.185	0.130	0.259	3.0					
H(12)	−0.149	0.109	0.362	3.0					
H(21)	0.044	0.432	0.052	3.0					
H(22)	1/8	0.348	0.024	3.0					
H(51)	−0.119	0.314	0.419	3.0					
H(52)	−0.052	0.411	0.372	3.0					
H(61)	0.073	0.145	−0.027	3.0					
H(62)	0.023	0.050	0.041	3.0					
H(111)	0.110	0.590	0.360	3.0					
H(112)	0.200	0.515	0.325	3.0					
H(121)	1/4	0.870	3/8	3.0					
H(122)	0.332	0.880	0.280	3.0					
H(141)	0.070	0.710	0.240	3.0					
H(142)	0.100	0.850	0.140	3.0					
H(161)	0.280	0.590	−0.050	3.5					
H(162)	0.360	1/2	−0.005	3.5					

[a] Estimated standard deviations in the least significant figure(s) are given in parentheses in this and all subsequent tables. The form of the anisotropic thermal ellipsoid is $\exp[-(B_{11}h^2 + B_{22}k^2 + B_{33}l^2 + 2B_{12}h_k + 2B_{13}H_l + 2B_{23}k_l)$. The quantities given in the table are the thermal coefficients × 10^3.

Table III. Interatomic Distances in the Metal Atom Environments

Ni(1)–O(1)	2.034 (5)	Ni(1)–O(4)	2.075 (5)
Ni(1)–O(2)	2.078 (4)	Ni(1)–N(1)	2.070 (6)
Ni(1)–O(3)	2.056 (5)	Ni(1)–N(2)	2.098 (6)
Ni(2)–O(5)	2.053 (5)	Ni(2)–W(2)	2.064 (5)
Ni(2)–O(6)	2.057 (5)	Ni(2)–W(3)	2.068 (5)
Ni(2)–W(1)	2.089 (5)	Ni(2)–W(4)	2.066 (6)

in the isostructural compounds (notice that the *R* factor of the present structural study is rather low). The average Ni(2)–O distance is 2.066 Å. The most important distortion affects the bond angles in which are implied the bridging oxygens O(5) and O(6): O(5)Ni(2)O(6) = 97.2 (2)°, O(5)Ni(2)W(3) = 85.4 (2)°, and O(6)Ni(2)W(4) = 83.2 (2)°.

The above species ((Ni(1)EDTA) and $(Ni(2)(H_2O)_4O_2)$ sharing two oxygen atoms O(5) and O(6) of distinct carboxylate groups alternate in order to form infinite zigzag chains (Figure 3), the general features of which may be described from "triangles" Ni(1)–Ni(2)–Ni(1).

In Table IV are listed the characteristic parameters of these "triangles" and bridging carboxylate angles; these are compared

Table IV. Distances (Å) between Metallic Sites in the Isostructural Series of the EDTA Complexes[a]

	[NiNi]	[CoCo][15]	[ZnZn][10]	[Mn–Cu][16] b	[Mn–Co][16] b	[Mg–Zn][16] b	[Ni–Ni][17] amorphous	
M(1)–M(2)^{i}	5.517 (3)	5.581	5.578	5.481	5.392	5.335	5.58	5.58
M(1)–M(2)^{v}	5.890 (7)	5.994	5.990	6.122	6.061	6.011	5.58	5.90
M(1)–M(1)^{iv}	7.305 (12)	7.377	7.377	7.424	7.409	7.370	7.05	7.45
O(1)–C(3)–O(5)	123.22	123.4	132	123.79	123.59	123.52		
O(2)–C(4)–O(6)	126.09	124.8	121	125.31	125.10	124.34		

[a] For the amorphous nickel complex, the two columns correspond to the limiting geometries. i = x, y, z; iv = $^1/_2 - x, ^1/_2 + y, ^1/_2 - z$; v = $-^1/_2 - x, ^1/_2 + y, ^1/_2 - z$. [b] M(1) = Cu, Co, Zn; M(2) = Mn, Mg.

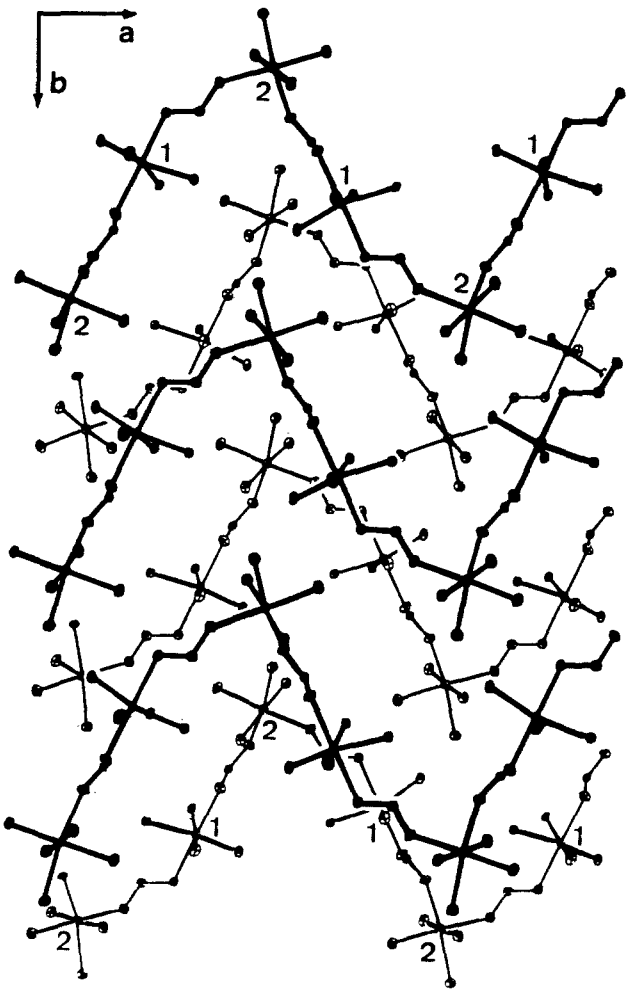

Figure 4. Stacking of the zigzag chains. For the sake of clarity, only the metal environments and the bridging carboxylate groups have been drawn. Ni(1)–EDTA sites and Ni(2)–$(H_2O)_4$ sites are labeled 1 and 2, respectively. The heavy lined chains are at mean $z = {}^3/_4$; the other ones are at mean $z = {}^1/_4$.

Table V. Shortest Intermolecular Distances (Å) within the Unit Cell[a]

O(1)–W(4)^{ii}	2.734 (7)	O(7)–W(3)^{vi}	2.832 (9)
O(3)–W(6)^{vi}	2.738 (8)	O(8)–W(3)^{ii}	2.708 (8)
O(4)–W(2)^{ii}	2.861 (7)	O(8)–W(1)^{vii}	2.754 (8)
O(7)–W(4)^{viii}	2.733 (8)		
W(1)–W(5)^{ix}	3.053 (10)	W(4)–W(5)^{ix}	3.007 (9)
W(2)–W(6)^{iii}	2.682 (8)		

[a] ii = $x, y-1, z$; iii = ${}^1/_2 - x, {}^1/_2 + y, {}^1/_2 + z$; vi = ${}^1/_2 - x, y - {}^1/_2, {}^1/_2 + z$; vii = ${}^1/_2 - x, y - {}^1/_2, z$; viii = $-x, 1-y, {}^1/_2 + z$; ix = $x - {}^1/_2, {}^3/_2 - y, z$.

with results from some isostructural compounds of the series $MM'(EDTA)(H_2O)_4,2H_2O$ and with the values computed for the amorphous (NiNi) complex.[17]

Notice, finally, that the zigzag chains hold together by hydrogen bonds and van der Waals interactions between oxygen atoms of the remaining free carboxylate groups and water molecules (see the distances in Table V).

Magnetic Results and Discussion

The complex under consideration displays a rounded maximum of susceptibility centered at $T \simeq 10$ K (Figure 5) and a Curie–Weiss behavior at higher temperatures. Such features agree with the presence of short-range antiferromagnetic interactions between Ni(II) ions. Owing to the structural stacking of the species

(17) Mosset, A.; Galy, J.; Coronado, E.; Drillon, M.; Beltran, D. *J. Am. Chem. Soc.* **1984**, *106*, 2864.

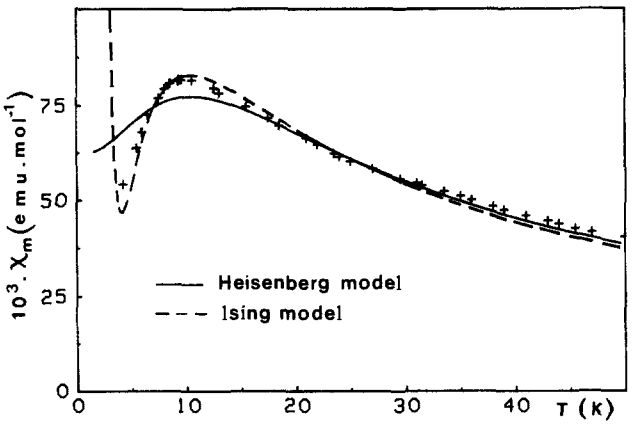

Figure 5. Magnetic behavior of $Ni_2(EDTA)(H_2O)_4,2H_2O$. The curves in full and dashed lines correspond to the Heisenberg and Ising models, respectively.

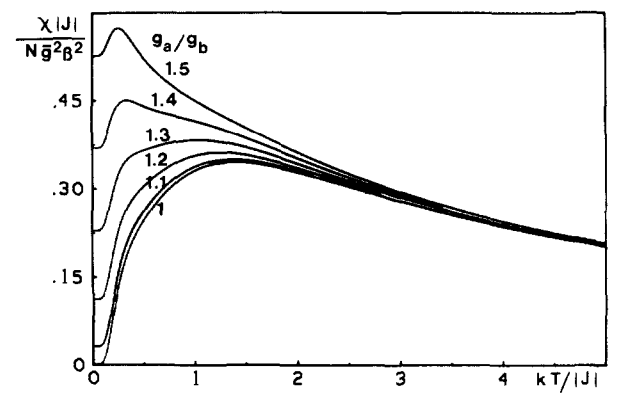

Figure 6. Heisenberg exchange-coupled chain. Normalized susceptibility per spin pair vs. $kT/|J|$ of an 8-spin ring for various values of the ratio between Landē factors.

Ni(1)EDTA and $Ni(2)(H_2O)_4O_2$, the complex may be viewed as a regular spin-1 chain with alternating Landē factors as follows:

$$...S(g_a)-S(g_b)-S(g_a)-S(g_b)...$$

Let us focus on the behavior of such a system on the basis of the symmetry of the exchange coupling.

(1) Theoretical of the Two-Sublattice Chain. We assume a spin-1 chain with an antiferromagnetic interaction between nearest neighbors. According to the dimensionality of the space available to quantum spins, the system may be described by a fully isotropic Hamiltonian (Heisenberg model) or an isotropic one favoring only an arbitrary z direction (Ising model). We report here the results of such treatments when alternating Landē factors are taken into account.

Heisenberg Model. Let S_i ($i = 1...2N$) be the current spin vector of a $2N$-site closed chain and g_a and g_b the Landē factors depending on site parity; the Hamiltonian to be solved is given by

$$\mathcal{H} = -J\sum_i \vec{S}_i S_{i+1} - (g_a\sum_i \vec{S}_{2i-1} + g_b\sum_i \vec{S}_{2i})\mu_B\vec{\mathcal{H}} \qquad (1)$$

where a negative J value refers to an antiferromagnetic coupling and cyclic boundary conditions impose $\vec{S}_{2N+1} = \vec{S}_1$.

For rings of $2N$ spins, the eigenvalue problem consists in solving a $(2S+1)^{2N}$ energy matrix. As previously shown,[7] a very significant reduction of the computational work is obtained by taking fully into account the geometrical (transition and mirror plane) and spin space symmetries of the $2N$-sites closed chain. This way, the calculations were performed up to 8-spin rings (the largest block matrix is then 66×66) with reasonable computing time on a UNIVAC 1110 machine.

For the uniform chain ($g_a = g_b$), the results correspond to those reported by Weng[2] (the treatment was limited to a 7-spin ring). As soon as g_a differs from g_b, nondiagonal terms of the Zeeman contribution arise, making the susceptibility computation a much more tedious work. Due to the noncompensation of the two

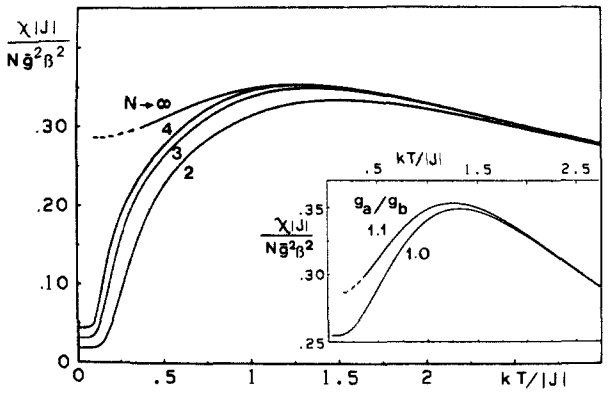

Figure 7. Heisenberg exchange-coupled chain. Normalized susceptibility of finite closed chains (length $2N$) computed for $g_a/g_b = 1.1$ that corresponds to the expected ratio in the nickel(II) complex.

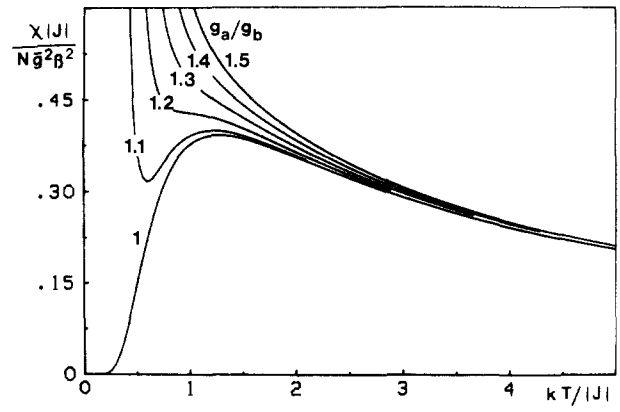

Figure 8. Normalized susceptibility of the Ising exchange-coupled chain for various values of the Landē factor sublattices.

sublattices, the behavior is expected to be similar to that of the alternating spin chain ($S_a \neq S_b$) previously reported. Then, we will refer to ferrimagnetic 1D systems.

The results are plotted in Figures 6 and 7 under the form of normalized susceptibility per spin pair vs. $kT/|J|$. Putting $\bar{g}^2 = (g_a^2 + g_b^2)/2$ allows one to obtain a uniform behavior in the high-temperature limit.

The influence of alternating g values reported for an 8-spin ring (Figure 6) appears to be particularly significant at low temperatures, giving a non-zero susceptibility as $T \rightarrow 0$ K. Further, the observed maximum is shifted toward low temperatures and increased in height.

For $g_a/g_b = 1.1$, which corresponds to the upper limit for the Ni(II) chain under consideration, the extrapolation of the curves to the thermodynamic limit ($N \rightarrow \infty$) is obtained from the polynomial

$$\chi_N = \chi_\infty + \sum_\eta a_\eta N^{-\alpha\eta} \qquad (2)$$

where a_η and α are depending on $kT/|J|$.

Owing to the site alternation, we have only considered rings of even parity approaching the limiting curve by lower values. Recall that for the uniform chain ($g_a = g_b$), the determination of the limiting behavior is easier, since it is approached monotonically by upper and lower values for odd and even parity rings, respectively. Due to the above considerations, it was of major significance to test the extrapolation law from the uniform $S = 1$ system.

The quality of the extrapolation becomes satisfying by assuming that the α's remain unchanged on going from $g_a/g_b = 1.0$ to 1.1. This way, we used a second-order polynomial. Then, the limiting curve ($N \rightarrow \infty$) drawn in Figure 7 corresponds to an accuracy better than 0.5% for $kT/|J| > 0.6$ and about 3% down to $kT/|J| = 0.2$. Any extrapolation at lower temperatures becomes unrealistic in this case. A comparison of the behaviors of regular ($g_a = g_b$) and alternating ($g_a = 1.1g_b$) chains is given in the inset. Notice that the maximum of susceptibility is slightly shifted in both coordinates. Further, the divergence of the susceptibility, common to all ferrimagnetic systems when approaching absolute zero, is expected at very low temperatures, only.

Ising Model. As previously shown,[18] most of the physical features of ferrimagnetic chains are elucidated from the $S_a = S_b = 1$ system with an altternation of Landē factors as well as anisotropy constants. The Hamiltonian may be expressed as

$$\mathcal{H} = -J\sum_i S_i^z S_{i+1}^z - D_a\sum_i (S_{2i-1}^z)^2 - D_b\sum_i (S_{2i}^z)^2 + H_{Zeem} \qquad (3)$$

where D_a and D_b are standard for local anisotropy constants and H_{Zeem} is given in eq 1. The problem may be solved exactly by the transfer matrix method which is convenient when the external magnetic field is applied along the quantization axis.[19] If Z is the partition function per pair of sites, this quantity is nothing but the largest eigenvalue of the transfer matrix $\mathbf{T}$ defined as

$$\mathbf{T} = \begin{pmatrix} s_a(s_b t^2 + x_b + s_b^{-1}t^{-2}) & s_a(s_b t + x_b + s_b^{-1}t^{-1}) & s_a(s_b + x_b + s_b^{-1}) \\ x_a(s_b t + x_b + s_b^{-1}t^{-1}) & x_a(s_b + x_b + s_b^{-1}) & x_a(s_b t^{-1} + x_b + t s_b^{-1}) \\ s_a^{-1}(s_b + x_b + s_b^{-1}) & s_a^{-1}(s_b t^{-1} + x_b + t s_b^{-1}) & s_a^{-1}(s_b t^{-2} + x_b + t^2 s_b^{-1}) \end{pmatrix}$$

where

$$t = \exp(J/kT) \qquad x_i = \exp(-D_i/kT)$$
$$s_i = \exp(g_i\mu_B\mathcal{H}/kT) \qquad \text{with } i = a, b \qquad (4)$$

If $U(\mathcal{H})$ is the largest root in a non-zero external magnetic field $\mathcal{H}$, $d^2/d\mathcal{H}^2(\ln U(\mathcal{H}))$ is closely related to the magnetic susceptibility. We readily obtain the zero-field susceptibility χ per spin pair:

$$\chi = \frac{2N\mu_B^2}{kT}\,\frac{\alpha_1 U(0) - \alpha_o}{3U^2(0) - 2\beta_1 U(0) + \beta_o} \qquad (5)$$

where the various coefficient are given by:

$$\alpha_o = 4x_a x_b((t-1)^2 g_+^2 + (1-t^{-1})^2 g_-^2) + (t-t^{-1})^2((x_a + x_b)(g_+^2 + g_-^2) + 2(x_a - x_b)g_+g_-)$$

$$\alpha_1 = (x_a + x_b)(g_+^2 + g_-^2) - 2(x_a - x_b)g_+g_- + 4(t^2 g_+^2 + t^{-2}g_-^2)$$

$$\beta_o = 2x_a x_b((1-t)^2 + (1-t^{-1})^2) + 2(x_a + x_b)(t - t^{-1})^2 + (t^2 - t^{-2})^2$$

$$\beta_1 = x_a x_b + 2(x_a + x_b) + 2(t^2 + t^{-2})$$

$$\text{with } g_+ = 1/2(g_a + g_b),\ g_- = 1/2(g_a - g_b) \qquad (6)$$

Let us look at Figure 8 where the curves $\chi|J|/N\bar{g}^2\beta^2$ vs $kT/|J|$ are drawn for several values of g_a/g_b whereas D_a and D_b are set equal to zero (no local anisotropy). The case $g_a/g_b = 1$ deals with the regular $S = 1$ antiferromagnetic chain previously studied by Obokata and Oguchi.[20] Conversely, for $g_a \neq g_b$ we obtain a typical 1D ferrimagnet for which the susceptibility (and the χT product) diverges at low temperatures. It is worth noticing that the maximum of $\chi = f(T)$ is conserved as long as g_a and g_b are quite close.

The influence of local anisotropy which gives rise to a lot of interesting physical situations, according to the sign and magnitude of the anisotropy parameters, was thoroughly investigated elsewhere.[18]

(2) Analysis of the Results. In a preliminary study it was shown that the regular Heisenberg chain model was not fully appropriate to explain the low-temperature magnetic behavior of the Ni(II) complex.[21] Clearly, the consideration of the Landē factor alternation may provide more insight, in the temperature range of

(18) Georges, R.; Curely, J.; Drillon, M. *J. Appl. Phys.* **1985**, *58*, 914.
(19) Kramers, H. A.; Wannier, G. H. *Phys. Rev.* **1941**, *60*, 252.
(20) Obokata, T.; Oguchi, T. *J. Phys. Soc. Jpn.* **1968**, *25*, 322.
(21) Beltran, D.; Escriva, E.; Drillon, M. *J. Chem. Soc., Faraday Trans.* **1982**, *78*, 1773.

interest, but also it may give a system over-parametrized so that we must keep cautious. This way, we have prepared the isostructural (MgNi) compound in which the Ni(II) ion occupies selectively the "quelated" position. Unfortunately, no signal has been observed by EPR measurement, probably due to the large distortion from the octahedral symmetry (preliminary specific heat studies suggest a large zero-filed splitting of the $^3A_2$ ground term). Nevertheless, an upper limit of g_a/g_b[24] can be assumed by refering to commonly observed g values for the Ni(II) ion in similar environments (varying between 2.1 and 2.4).[22] A least-squares refinement of the limiting curve ($N \rightarrow \infty$) (Figure 7) computed for $g_a/g_b = 1.1$ led to the rational expression

$$\frac{\chi|J|}{Ng^2\beta^2} = \frac{4x + 0.1864x^2 + 1.2084x^3}{3 + 4.7658x + 3.3652x^2 + 8.3403x^3} \quad (7)$$

where $x = |J|/kT$.

The agreement criterion defined as the sum of the squares of the relative deviations is $R = 1.6 \times 10^{-5}$. Using expression 7, the best agreement between theory and experiment (solid line in Figure 5) corresponds to $J = -8.35K$, $g_a = 2.31$, and $g_b = 2.10$. It is to be noticed that the description of the low-temperature susceptibility is not improved by introducing the g alternation. In particular, the experimental data decrease significantly when cooling down to zero by contrast with theoretical ones. Such a discrepancy could result from the local anisotropy effects, not introduced in the above model. Unfortunately, the theoretical treatment of the Heisenberg chain involving two distinct local distortions is not available today.

Anyway, it has been emphasized that a local anisotropy of the Ni(II) ions establishes a preference for the moments to align in a given direction[5] so that an anisotropic exchange model (Ising or XY-type) becomes relevant to analyze the magnetic behavior. Using the Ising model developed in the previous section, we show that the quality of the fit is greatly improved by only taking into account J, g_a, and g_b as adjustable parameters (dashed line in Figure 5); we obtain $J = -8.25K$, $g_a = 2.21$, and $g_b = 2.09$. Note that such a model gives a very good description of the rounded maximum and agrees with the data at lower temperatures. From a close examination, it does not seem necessary to introduce in the fit further parameters. This suggests that the anisotropic exchange model is convenient to describe the competition between anisotropy effects and exchange coupling in the temperature range of interest.

(22) McGarvey, B. R. *Transition Met. Chem. (Weinheim, Ger.)* **1966**, *3*, 89.

Conclusion

We have discussed in this paper the behavior of an $S = 1$ chain characterized by alternating Landé factors. So far, the 1D ferrimagnetic character was related to the presence of two noncompensated spin sublattices. We show, here, that the alternation of Landé factors gives rise to the same divergence of susceptibility when $T \rightarrow 0$ K (ferrimagnetic chains).

Two exchange models were developed to describe the behavior of the $Ni_2(EDTA)(H_2O)_4,2H_2O$ complex, namely the Heisenberg and Ising models.

The former was shown to give a poor agreement with experiment in spite of the consideration of alternating g factors. Clearly, the analysis of the $\chi = f(T)$ variation is greatly improved by using the fully anisotropic (Ising) model. In fact, further effects could be invoked in order to explain the decrease of susceptibility below $T = 10$ K, as for instance magnetic interactions between neighboring chains. Specific heat studies down to 0.1 K have shown that this effect should be negligeable in the present system.[23] Finally, it is to be underlined that the slight inequality between consecutive Ni–Ni distances, related to different bridging carboxilate angles (see Table IV), could result in a J-alternating chain. A complete treatment involving this last effect is in progress.

Acknowledgment. This work was partly supported by the CAICYT and by the "Programme d'actions intégrées franco-espagnoles".

Registry No. (NiNi), 99687-31-7.

Supplementary Material Available: Listings of structure factor amplitudes (10 pages). Ordering information is given on any current masthead page.

(23) de Jongh, J., private communication.

(24) In agreement with crystal field parameters of the two Ni(II) ions (D = 1030 and 820 cm^{-1} for the "chelated" and "hydrated" site, respectively) the larger g value (g_a) may be associated to the "hydrated" site.

Ultraviolet Resonance Raman Characterization of Photochemical Transients of Phenol, Tyrosine, and Tryptophan

Craig R. Johnson, Michael Ludwig, and Sanford A. Asher*

Contribution from the Department of Chemistry, University of Pittsburgh, Pittsburgh, Pennsylvania 15260. *Received July 26, 1985*

Abstract: Ultraviolet resonance Raman (UVRR) spectra of solutions of phenol, tyrosine, and tryptophan at pH 7 and 12 show Raman bands that are assigned to the photoionization products phenoxy, tyrosyl, and tryptophanyl radicals, respectively. These photoinduced transients are only detected at high laser power densities (high average power, tightly focused, pulsed-laser excitation) when exciting within the $\pi \rightarrow \pi^*$ transitions of the precursor compounds. Each of the radicals show UVRR spectra distinct from their precursors. A pump–probe experiment shows that the phenolate transient (phenoxy radical) produced by the incident laser beam at pH 12 has a lifetime significantly longer than 10 ns. The dependence of the Raman scattering intensity upon incident laser-power density is consistent with a simple model in which the free radical is produced by a monophotonic photoionization process. Saturation effects are also evident at high power densities. Photochemistry, absorption band optical saturation, and nonlinear optical processes are proven and potential impediments for measurements of Raman spectra and excitation profiles with pulsed laser excitation. On the other hand, the facile production and detection of free radical species with UVRR suggest that this technique will be useful in the investigation of radical structure and chemistry.

Several major research efforts,[1-3] in addition to our own, are under way to extend the study of resonance Raman excitation profiles into the ultraviolet and vacuum-ultraviolet[4] spectral regions. Much of this work is directed toward the application of

0002-7863/86/1508-0905$01.50/0